



HAL
open science

Structural and Functional Analysis of the Metal-binding Sites of *Clostridium thermocellum* Endoglucanase CelD

Sylvie Chauvaux, H el ene Souchon, Pedro Alzari, Patrick Chariot, Pierre Beguin

► **To cite this version:**

Sylvie Chauvaux, H el ene Souchon, Pedro Alzari, Patrick Chariot, Pierre Beguin. Structural and Functional Analysis of the Metal-binding Sites of *Clostridium thermocellum* Endoglucanase CelD. *Journal of Biological Chemistry*, 1995, 270 (17), pp.9757-9762. 10.1074/jbc.270.17.9757 . pasteur-03136564

HAL Id: pasteur-03136564

<https://pasteur.hal.science/pasteur-03136564>

Submitted on 9 Feb 2021

HAL is a multi-disciplinary open access archive for the deposit and dissemination of scientific research documents, whether they are published or not. The documents may come from teaching and research institutions in France or abroad, or from public or private research centers.

L'archive ouverte pluridisciplinaire **HAL**, est destin ee au d ep ot et  a la diffusion de documents scientifiques de niveau recherche, publi es ou non,  emanant des  tablissements d'enseignement et de recherche fran ais ou  trangers, des laboratoires publics ou priv es.



Distributed under a Creative Commons Attribution 4.0 International License

Structural and Functional Analysis of the Metal-binding Sites of *Clostridium thermocellum* Endoglucanase CelD*

(Received for publication, January 31, 1995)

Sylvie Chauvaux‡, H el ene Souchon§, Pedro M. Alzari§, Patrick Chariot¶, and Pierre Beguin‡||

From the ‡Unit  de Physiologie Cellulaire and URA 1300 CNRS, D epartement des Biotechnologies and the §Unit  d'Immunologie Structurale and URA 359 CNRS, D epartement d'Immunologie, Institut Pasteur, 28 rue du Dr Roux, 75724 Paris Cedex 15, France and the ¶Service de Pharmacologie et Toxicologie, H opital Henri-Mondor, 51 Avenue de Lattre de Tassigny, 94010 Cr eteil, France

Crystallographic analysis indicated that *Clostridium thermocellum* endoglucanase CelD contained three Ca²⁺-binding sites, termed A, B, and C, and one Zn²⁺-binding site. The protein contributed five, six, and three of the coordinating oxygen atoms present at sites A, B, and C, respectively. Proteins altered by mutation in site A (CelD_{D246A}), B (CelD_{D361A}), or C (CelD_{D523A}) were compared with wild type CelD. The Ca²⁺-binding isotherm of wild type CelD was compatible with two high affinity sites ($K_a = 2 \times 10^6 \text{ M}^{-1}$) and one low affinity site ($K_a < 10^5 \text{ M}^{-1}$). The Ca²⁺-binding isotherms of the mutated proteins showed that sites A and B were the two high affinity sites and that site C was the low affinity site. Atomic absorption spectrometry confirmed the presence of one tightly bound Zn²⁺ atom per CelD molecule. The inactivation rate of CelD at 75  C was decreased 1.9-fold upon increasing the Ca²⁺ concentration from 2×10^{-5} to 10^{-3} M. The K_m of CelD was decreased 1.8-fold upon increasing the Ca²⁺ concentration from 5×10^{-6} to 10^{-4} M. Over similar ranges of concentration, Ca²⁺ did not affect the thermostability nor the kinetic properties of CelD_{D523A}. These findings suggest that Ca²⁺ binding to site C stabilizes the active conformation of CelD in agreement with the close vicinity of site C to the catalytic center.

Clostridium thermocellum synthesizes a multienzymatic cellulase complex with a molecular mass of 2–4 MDa, termed cellulosome (1, 2). Endoglucanase CelD is a component of the cellulosome, which can be easily purified in large amounts from inclusion bodies produced in recombinant *Escherichia coli* (3). CelD belongs to the family E of cellulases (4, 5). The three-dimensional structure of CelD¹ has been determined by x-ray crystallography (6). The protein contains two distinct structural domains that are closely associated: a small amino-terminal β -barrel domain and a larger, mostly α -helical domain, whose amino acid sequence is similar in all catalytic domains of family E cellulases (4, 7). The COOH terminus of CelD consists of a duplicated segment of 23 residues that is involved in anchoring the protein to the scaffolding component of the cellulosome (8, 9). The part of the protein visible in the electron density map terminates 10 residues upstream from the begin-

ning of the COOH-terminal duplication. A cleft on the surface of the α -helical domain constitutes the active site. According to structural analysis (6) and mutagenesis data (10), the two residues participating in acid-base catalysis are Asp-201 and Glu-555.

We have previously shown that Ca²⁺ binds to CelD, thereby stabilizing the enzyme against thermal denaturation and increasing its substrate binding affinity (11). Three putative Ca²⁺-binding sites and one putative Zn²⁺-binding site were identified in the catalytic domain of the CelD crystal structure (6).

This paper reports the structural analysis of the Zn²⁺-binding site and of the three Ca²⁺-binding sites of *C. thermocellum* CelD. The presence of Zn²⁺ in CelD was assayed by atomic absorption spectrometry. CelD proteins carrying mutations in each of the Ca²⁺-binding sites were purified and characterized to assess the contribution of each site to Ca²⁺ binding. The rate of inactivation at 75  C and the kinetic parameters of wild type CelD were determined in the presence of varying Ca²⁺ concentrations to correlate changes in these parameters with the occupancy of high or low affinity Ca²⁺-binding sites. The same assays were performed with CelD mutated in the low affinity Ca²⁺-binding site.

MATERIALS AND METHODS

Crystallographic Analysis—Two isomorphous crystal forms of CelD were grown using ammonium sulfate (*i.e.* no added calcium) or 300 mM calcium chloride as precipitants. Structure determination and independent refinement of the two forms at 2.3   resolution have been described elsewhere (6). The present models comprise residues 36–574 and include three calcium ions, one zinc ion, and 221 (ammonium sulfate) or 204 (calcium chloride) water molecules. The final agreement factors between observed and calculated structure factor amplitudes in the resolution range 6–2.3   were 17.0% for 33,211 observed reflections with $F > 5 \sigma(F)$ (ammonium sulfate) and 17.4% for 29,797 observed reflections (calcium chloride). Root mean squares deviations of bond lengths and angles from ideality were 0.007   and 1.6 , respectively, in both crystal structures.

Bacterial Strains and Plasmids—Plasmids pCT6523, pCT6525, and pCT6527, encoding the catalytic domain of CelD and carrying the D246A, D361A, and D523A mutations, respectively, were previously obtained (10). Each of the mutations was inserted into a plasmid whose sequence included the 3'-end of *celD*, as previously described (10). The resulting plasmids, carrying the D246A, D361A, and D523A mutations, were termed pCT6543, pCT6545, and pCT6547, respectively. The isogenic plasmid, pCT6540, encoding the wild type enzyme, has been described (10).

The pCT6540 and pCT6547 plasmids were harbored by *E. coli* TG1 (12) = K-12, $\Delta(lac-proAB)$, *thi*, *supE*, *hsdD5* (*F'* *traD36*, *proAB*⁺, *lacI*^q, *lacZ* Δ M15). pCT6543 and pCT6545 were harbored by *E. coli* JM101 (13) = K-12, $\Delta(lac-proAB)$, *thi*, *supE* (*F'* *traD36*, *proAB*⁺, *lacI*^q, *lacZ* Δ M15).

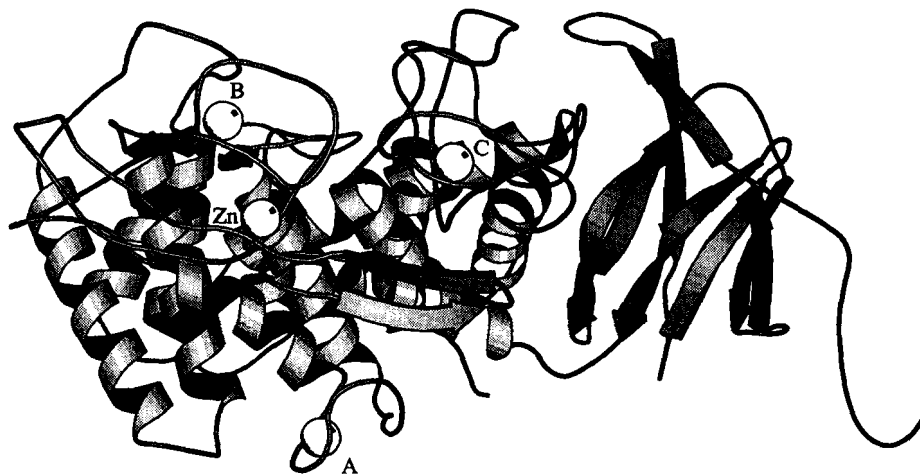
Purification of Wild Type and Mutant Forms of CelD—*E. coli* cells harboring the appropriate plasmids were grown to stationary phase at 37  C in Luria Bertani broth (14) containing 100 $\mu\text{g/ml}$ ticarcillin. Wild type and mutant forms of CelD were purified from inclusion bodies as previously described (3). Low and high M_r forms of CelD_{D246A} (CelD-A*)

* This work was supported by Contract AIR1-CT-0321 from the Commission of the European Communities and by research funds from the University of Paris 7. The costs of publication of this article were defrayed in part by the payment of page charges. This article must therefore be hereby marked "advertisement" in accordance with 18 U.S.C. Section 1734 solely to indicate this fact.

|| To whom correspondence should be addressed.

¹ The abbreviations used are: CelD, endoglucanase CelD; PAGE, polyacrylamide gel electrophoresis; MOPS, 3-(*N*-morpholino)propane-sulfonic acid; *p*-NPC, *p*-nitrophenyl- β -D-cellobioside.

FIG. 1. Metal-binding sites of endoglucanase CelD. The polypeptide chain is indicated by a ribbon diagram. α -Helices are indicated by wound ribbons, and β -strands are indicated by arrows. Metal ions are shown as white spheres. A, B, and C, Ca^{2+} -binding sites; Zn, Zn^{2+} -binding site. The diagram was drawn with MOLSCRIPT (21).



and CelD_{D361A} (CelD-B*) were separated on a Mono-Q anion exchange column using a fast performance liquid chromatography system (Pharmacia Biotech Inc.). Up to 4 mg of purified protein was loaded on a Mono-Q HR5/5 anion exchange column (1 ml) equilibrated with 20 mM Tris-HCl, pH 7.7, at a rate of 1 ml/min. Elution was performed at 0.7 ml/min using a linear gradient from 100 to 220 mM NaCl in the same buffer. The low M_r and high M_r peaks were eluted at 150 and 180 mM NaCl, respectively, and concentrated by ultrafiltration using a YM10 Amicon membrane. All samples were dialyzed against 40 mM Tris-HCl, pH 7.7.

Protein Electrophoresis—SDS-PAGE was performed according to Laemmli (15). Samples were boiled for 5 min in 2% SDS, 10% glycerol, 5% β -mercaptoethanol, 62.5 mM Tris-HCl, pH 6.8. Non-denaturing PAGE was performed using the same procedure, omitting SDS and β -mercaptoethanol and the heat treatment of the samples.

Zinc Assay—The zinc content of wild type CelD was assayed by flame atomic absorption spectroscopy at 213.9 nm using a Varian AA-1275 spectrophotometer (Varian Techtron, Springvale, Australia), with a single element hollow-cathode lamp for zinc (16).

Ca^{2+} -binding Assay—Binding of ^{45}Ca to purified proteins was assayed by monitoring the release of ^{45}Ca from Chelex-100 (Bio-Rad) previously equilibrated with various concentrations of ^{45}Ca (11).

Enzyme and Protein Assays—All reagents used in assays performed in the presence of controlled concentrations of Ca^{2+} were kept in disposable plasticware (Sterilin) and were handled with disposable plastic pipettes or pipette tips. Divalent metals were removed from 50 mM Na-MOPS buffer, pH 6.3, and from 20 mM *p*-NPC, dissolved in the same buffer, by shaking with 10% (w/v) Chelex-100. The resin was removed by centrifuging at $1,000 \times g$ for 2 min. Ca^{2+} was removed from CelD by shaking in the presence of 10% Chelex-100 followed by decantation. Alternatively, the enzyme was diluted in Chelex-treated buffer so that the contribution of protein-bound Ca^{2+} in the assay medium was less than 5×10^{-8} M, assuming 3 mol of Ca^{2+} bound/mol of CelD. No difference was observed between the results obtained with either procedure, even when no Ca^{2+} was added (data not shown).

Enzyme activity was assayed at 60 °C in 50 mM Na-MOPS buffer, pH 6.3, containing CaCl_2 , EGTA, or ZnCl_2 as indicated for each experiment and 0.5–20 mM *p*-NPC as substrate. The reaction was stopped after less than 5% of the substrate had been hydrolyzed by adding $\frac{1}{3}$ vol 1 M Na_2CO_3 . 1 unit of activity is defined as the amount of enzyme liberating 1 μmol of *p*-nitrophenol ($\epsilon = 1.61 \times 10^4 \text{ cm}^2 \times \text{mol}^{-1}$) per min. Protein concentration was measured using the Coomassie Blue reagent supplied by Bio-Rad (17), with bovine serum albumin as a standard.

Thermostability—Proteins were either treated with Chelex-100 or diluted so that their contribution to the concentration of Ca^{2+} in the inactivation reaction was less than 1.5×10^{-7} M. No difference was observed between the results obtained with either procedure, even when no Ca^{2+} was added (data not shown).

Proteins were incubated at 75 °C at a concentration of 3–5 10^{-8} M in 50 mM MOPS buffer, pH 6.3, containing CaCl_2 , EGTA, or ZnCl_2 as indicated for each experiment. Temperature control was ascertained by checking the temperature inside of a plastic vial similar to those in which the inactivation reaction was performed. Samples were withdrawn at several time intervals and chilled on ice, and ZnCl_2 and CaCl_2 were added to a final concentration of 1 mM (2 mM CaCl_2 in the case of samples containing 1 mM EGTA). Residual activity was assayed as

described above, using 0.9 mM *p*-NPC.

Computations—Kinetic constants (including the 95% confidence interval) for the rate of inactivation were computed from linear regressions of log (residual activity) versus time, using the Instat Mac® program (version 2.0, GraphPad Software). K_m and k_{cat} values were calculated by non-linear regression using the KaleidaGraph® program (version 2.1, Abelbeck Software).

RESULTS

Crystallographic Analysis of Ca^{2+} -binding Sites in CelD—The three-dimensional structure of CelD revealed four metal-binding sites occupied by atoms heavier than water in the crystal. A first internal site is located immediately behind a protein loop involved in substrate binding and catalysis (Zn sphere in Fig. 1). The tetrahedral coordination by two Cys and two His side chains and the displacement by Hg suggests that this site is occupied by a Zn^{2+} ion (6). The three other metal binding sites are located close to the molecular surface in different regions of the protein (spheres A, B, and C in Fig. 1). From the coordination geometry, these three positions could be identified as Ca^{2+} -binding sites.

The coordination of the Ca^{2+} ion bound at site A appears as a slightly distorted octahedral arrangement with a water molecule at one of the vertices (Fig. 2A). Protein groups donate the five other oxygen ligands: two main chain carbonyls at positions 236 and 241 and the side chains of residues Asn-239, Asp-243, and Asp-246. The loop forming this site protrudes into the solvent and appears to be stabilized by calcium.

Seven oxygen atoms chelate the Ca^{2+} ion at site B. In this case, the coordination polyhedron appears as a distorted pentagonal bipyramid with Asp-362 and a main chain carbonyl at position 401 on the vertices, or alternatively as a distorted octahedral arrangement with one bidentate ligand, Asp-361 (Fig. 2B). In addition to the aspartate residues, protein oxygens involved in Ca^{2+} binding include the side chain of Thr-356 and the main chain carbonyl groups at positions 358 and 401. As shown in Fig. 2B, this site appears to have a structural role in linking together two different regions of the protein.

The protein loop forming site C is completely exposed to the solvent, with three out of the six oxygen ligands donated by water molecules (Fig. 2C). Main chain carbonyls at positions 520 and 525 and the carboxylate group of Asp-523 complete the calcium coordination polyhedron. Unlike sites A and B, the protein loop forming binding site C is partially involved in intermolecular interactions in the crystal. The side chain of Arg-314 from a neighbor molecule is stacked against Trp-526, and the carbonyl group at position 524 forms an intermolecular hydrogen bond with the guanido group of Arg-416 (data not shown).

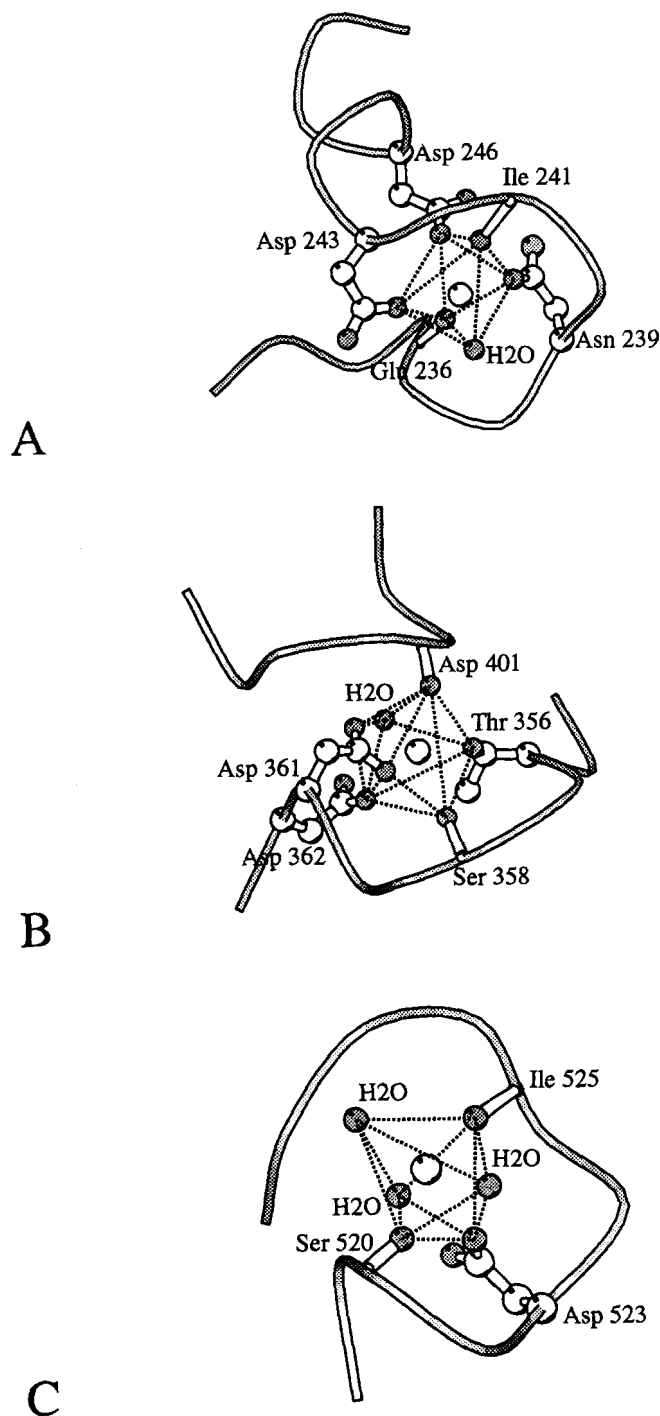


FIG. 2. Coordination polyhedra of the three Ca^{2+} -binding sites. The course of the polypeptide chain is indicated by a smooth tracing. Liganded groups (side chain residues, main chain carbonyls, water molecules) are indicated explicitly. Oxygen and nitrogen atoms are in gray. Ca^{2+} is drawn as a larger sphere inside of the coordination polyhedron. A, site A; B, site B; C, site C. Diagrams were drawn with MOLSCRIPT (21).

Sites B and C are close to either end of the substrate-binding groove and are expected to have some influence on the catalytic activity of CelD. On the opposite site of the α -barrel, the Ca^{2+} ion bound at site A stabilizes a helix-connecting loop with no obvious role in enzymatic activity. As a general rule, the conformation of the loops forming the three Ca^{2+} -binding sites does not follow the EF-hand pattern observed in many Ca^{2+} -binding proteins (18). Moreover, they differ significantly from

TABLE I
Interatomic distances in \AA between Ca^{2+} ions and protein oxygen atoms in CelD crystals grown in the presence of ammonium sulfate (form I) or calcium chloride (form II) as precipitants

Calcium binding site	Contact residue	Oxygen atom	Distance	
			Form I	Form II
A	Glu-236	O (main chain)	2.44	2.36
	Asn-239	O_5	2.38	2.35
	Ile-241	O (main chain)	2.48	2.37
	Asp-243	O_5	2.49	2.48
	Asp-246	O_5	2.67	2.69
B	Thr-356	O_γ	2.31	2.38
	Ser-358	O (main chain)	2.60	2.58
	Asp-361	$\text{O}_{\delta 1}$	2.69	2.68
	Asp-361	$\text{O}_{\delta 2}$	2.70	2.82
	Asp-362	O_5	2.60	2.48
	Asp-401	O (main chain)	2.40	2.43
C	Ser-520	O (main chain)	2.29	2.30
	Asp-523	O_5	2.71	2.61
	Ile-525	O (main chain)	2.27	2.28

each other in loop conformation as well as in the side chains and the number of water molecules involved in the coordination polyhedra.

Overall, only small structural differences were observed for the structure of CelD at 0 and 300 mM calcium. The coordination geometry of the three sites was essentially the same within experimental error (Table I). Only the temperature factors of the calcium atoms bound at sites A and C were different in the two crystal forms (the temperature factors for the three calcium atoms were 27, 25, and 32 \AA^2 , respectively, at 300 mM CaCl, and 43, 28, and 47 \AA^2 at 0 mM CaCl), suggesting partial calcium occupancy of sites A and C in ammonium sulfate-grown crystals.

The D246A, D361A, and D523A mutations were chosen to inactivate Ca^{2+} -binding sites A, B, and C, respectively. The corresponding proteins will be termed CelD-A*, CelD-B*, and CelD-C*, respectively.

Separation of High and Low M_r Forms of CelD-A* and CelD-B*—SDS-PAGE analysis indicated that the wild type and the three mutant proteins were mainly composed of 65-kDa CelD, with 68- and 63-kDa CelD being present as minor species in some of the preparations (Fig. 3A). Previous work has shown that proteolysis accounts for some heterogeneity of the COOH terminus of CelD. However, cleavage does not affect the catalytic domain of the protein, and the 68-, 65-, and 63-kDa species were shown to share very similar catalytic properties (9, 11, 19).

In non-denaturing electrophoresis (Fig. 3B), CelD-C* displayed the same mobility as wild type CelD, which is a monomeric protein (3). However, CelD-A* and CelD-B* could be separated into a form with a mobility similar to that of the wild type monomer and a slower migrating, higher M_r form, presumably resulting from self-association. The two forms could be separated by ion exchange chromatography on a Mono-Q column (Fig. 3B) or by gel filtration on a TSK G2000 column (data not shown) but tended to reequilibrate over a period of a few days. This explains the partial contamination of one form by the other seen in Fig. 3B.

Presence of Zn^{2+} —Atomic absorption spectroscopy showed the presence of 1.0 ± 0.2 mol of Zn^{2+} /mol of wild type CelD. No change in Zn^{2+} content was detected when the enzyme was incubated for 15 min at room temperature or at 60°C in the presence of 10% (w/v) Chelex-100, but incubation with Chelex at 75°C for 9 min resulted in total loss of detectable enzyme-

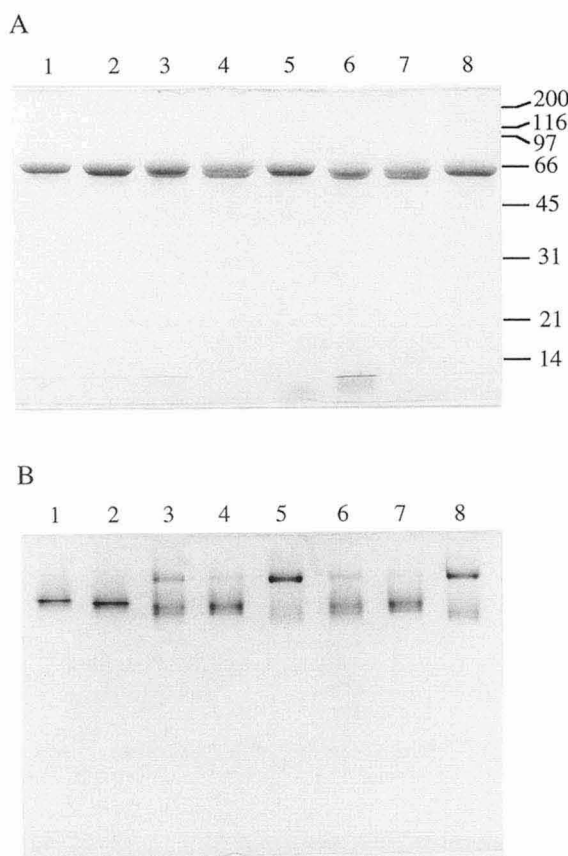


FIG. 3. Electrophoretic analysis of wild type and mutant forms of CelD. 4 μ g of each purified protein were analyzed by SDS-PAGE (panel A) and by non-denaturing PAGE (panel B). Lane 1, CelD; lane 2, CelD-C*; lane 3, CelD-A*; lane 4, monomeric form of CelD-A*; lane 5, high M_r form of CelD-A*; lane 6, CelD-B*; lane 7, monomeric form of CelD-B*; lane 8, high M_r form of CelD-B*. The migration and molecular mass of rabbit myosin (200 kDa), *E. coli* β -galactosidase (116 kDa), rabbit phosphorylase B (97 kDa), bovine serum albumin (66 kDa), ovalbumin (45 kDa), soybean trypsin inhibitor (21 kDa), and hen egg white lysozyme (14 kDa) are indicated on the right of panel A.

bound Zn^{2+} (data not shown). Dissociation of Zn^{2+} was correlated with an increase in the inactivation rate of the protein (see below).

Ca^{2+} -Binding Parameters—Fig. 4 shows the Scatchard analysis of Ca^{2+} binding to the wild type and various mutant forms of CelD. The binding isotherm of wild type CelD was compatible with the presence of two high affinity sites ($K_a = 2 \times 10^6 M^{-1}$) and one low affinity site ($K_a = 0.66 \times 10^5 M^{-1}$) per molecule. CelD-A* (Fig. 4A) and CelD-B* (Fig. 4B) each displayed one high affinity site with $K_a = 5.1 \times 10^6 M^{-1}$ and $K_a = 3.2 \times 10^6 M^{-1}$, respectively. CelD-C* displayed two high affinity sites with $K_a = 3.1 \times 10^6 M^{-1}$ (Fig. 4C). By contrast to the wild type, no low affinity site was detected in any of the mutant CelD proteins. Ca^{2+} -binding isotherms were the same for the low and high M_r forms of CelD-A* and CelD-B* (Fig. 4, A and B).

Effect of Ca^{2+} on Kinetic Parameters—Previous data indicated that Ca^{2+} decreased the K_m but had little effect on the k_{cat} of CelD (11). Fig. 5A confirms that addition or removal of Ca^{2+} had little effect on the k_{cat} of CelD and indicates that the strongest decrease in K_m (from 6.2 to 3.5 mM) occurred when the Ca^{2+} concentration was increased from 5×10^{-6} to 10^{-4} M. As a consequence, there was a concomitant increase in catalytic efficiency k_{cat}/K_m . Addition of 1 mM EGTA had little effect on CelD after Ca^{2+} ions had been removed by dilution in Ca^{2+} -free buffer. Fig. 5B shows that the kinetic parameters of CelD-C*

were not affected by EGTA nor by Ca^{2+} in the range of concentrations tested.

Thermostability—Fig. 6 shows the kinetic rate of inactivation k_{inact} of wild type CelD and of CelD-C* incubated at 75 °C in the presence of 1 mM EGTA or various Ca^{2+} concentrations. Addition of 1 mM EGTA in the inactivation reaction after Ca^{2+} ions had been removed by dilution in Ca^{2+} -free buffer or by Chelex treatment at room temperature resulted in a 2.4-fold increase in the rate of inactivation of both enzymes. Addition of Chelex-100 at 75 °C produced a similar effect (data not shown).

For the wild type enzyme, increasing the concentration of Ca^{2+} up to 5×10^{-5} M had no significant effect on the rate of inactivation. However, a 1.8-fold decrease in k_{inact} was observed upon increasing the concentration of Ca^{2+} from 5×10^{-5} to 10^{-3} M. Over the same range of Ca^{2+} concentration, the inactivation rate of CelD-C* was not affected.

DISCUSSION

The presence of one Zn^{2+} ion/mol of CelD, predicted from the crystallographic analysis of the protein, was confirmed by biochemical analysis. Zn^{2+} binding appeared quite stable at room temperature and at 60 °C, and dissociation of Zn^{2+} at 75 °C was accompanied by rapid denaturation of the enzyme. By contrast, Ca^{2+} could be dissociated from CelD without denaturing the protein.

Previous interpretation of Ca^{2+} binding data had led to the conclusion that CelD contained two high affinity Ca^{2+} -binding sites (11). Points extending beyond two sites/molecule in the Scatchard plots were not considered in the analysis. However, crystallographic analysis revealed the presence of three putative Ca^{2+} -binding sites in CelD (6). The presence of three functional Ca^{2+} -binding sites was confirmed by the analysis of CelD-C*, whose mutation affects site C. The Ca^{2+} -binding isotherm of CelD-C* displayed two high affinity sites similar to those of the wild type, but, in contrast to the wild type, binding did not exceed 2.1 mol of Ca^{2+} bound/mol of protein. This suggests that in the wild type, points extending between 2 and 3 mol of Ca^{2+} bound/mol of protein were due to the presence of site C, which behaved like a low affinity site. High affinity Ca^{2+} binding to sites A and B was confirmed by analysis of CelD-A* and CelD-B*. The Ca^{2+} -binding isotherms of both proteins showed that each mutation abolished high affinity binding to one site. The relative affinities of sites A, B, and C were consistent with the fact that in sites A and B, the protein contributes five and six, respectively, of the coordinating oxygens but only three of the coordinating oxygens of site C.

Mutagenesis of site A or B seemed to abolish binding to site C, as if site C could form only when both sites A and B are occupied. Why this should be the case is not obvious from structural analysis.

Investigation of the kinetic parameters of CelD indicated that the change in K_m of the enzyme as a function of the Ca^{2+} concentration was strongest between 5×10^{-6} and 10^{-4} M. This range is most likely accounted for by the increased occupancy of the low affinity site C rather than the high affinity sites A and B. The fact that the kinetic parameters of CelD-C* were not affected by Ca^{2+} confirms this interpretation.

The stabilization of wild type CelD occurred at concentrations that were an order of magnitude higher than those required to affect catalytic parameters. This may be explained by the fact that changes in catalytic properties induced by Ca^{2+} dissociation are reversible, whereas thermal denaturation is not. The Ca^{2+} concentrations at which stabilization was observed were consistent with a requirement for occupancy of site C rather than site A and B. Accordingly, inactivation of site C abolished Ca^{2+} -induced stabilization of CelD.

FIG. 4. Scatchard analysis of Ca^{2+} binding to wild type and mutant forms of CelD. Binding of ^{45}Ca ($5 \times 10^{-8} \text{ M} < (\text{CaCl}_2) < 2.5 \times 10^{-5} \text{ M}$) to $1.7 \times 10^{-5} \text{ M}$ purified protein is shown. Each point was the average of a duplicate determination. Closed circles, wild type CelD; open circles, monomeric mutant CelD; x, high M_r form of mutant CelD. Panel A, CelD-A*; panel B, CelD-B*; panel C, CelD-C*. The curve fitting the data for the wild type was drawn assuming that the enzyme contained two sites with a K_d of $2 \times 10^6 \text{ M}^{-1}$ and one site with a K_d of $0.66 \times 10^6 \text{ M}^{-1}$.

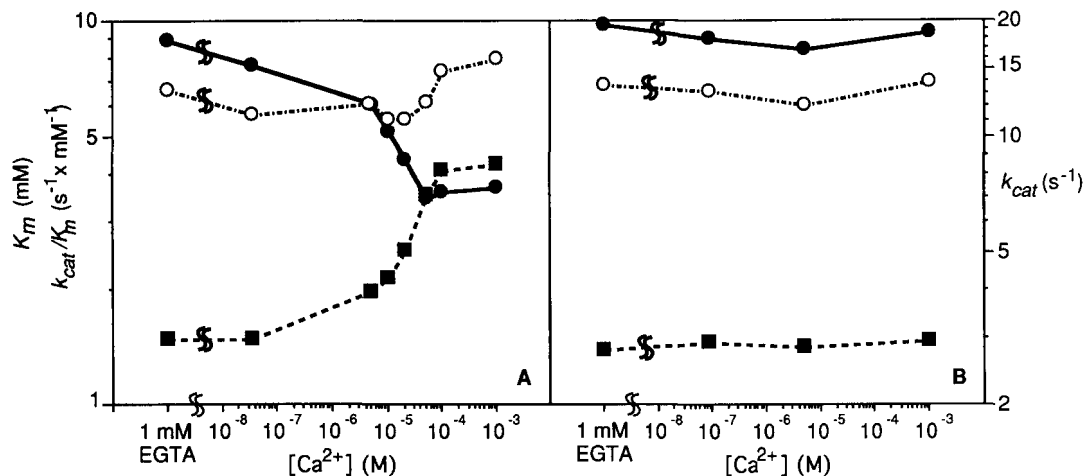
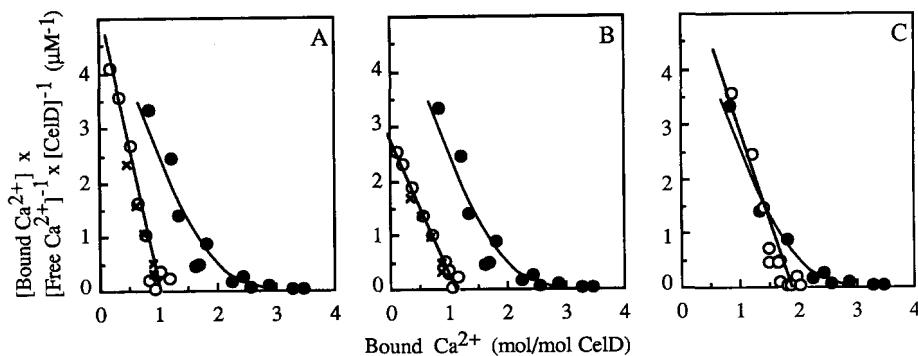


FIG. 5. Kinetic parameters of wild type CelD and CelD-C* as a function of divalent metal concentration. Results are presented using double logarithmic scales. Panel A, wild type CelD; panel B, CelD-C*. Open circles, k_{cat} ; closed circles, K_m ; closed squares, k_{cat}/K_m . The lowest Ca^{2+} concentration was calculated from the contribution of Ca^{2+} initially bound to the enzyme added to the assay. Except for the EGTA-treated samples, all samples contained $1 \mu\text{M}$ ZnCl_2 in addition to the Ca^{2+} concentrations indicated.

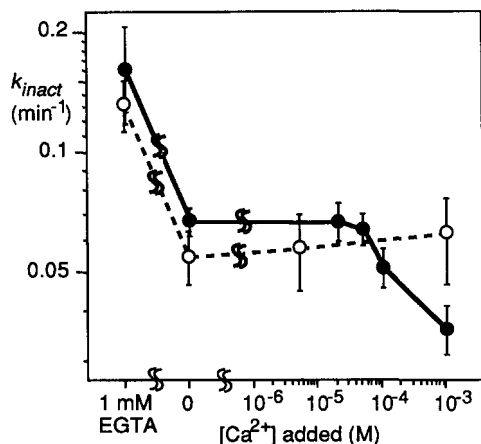


FIG. 6. Inactivation rate k_{inact} at 75°C of wild type CelD and CelD-C* as a function of divalent metal concentration. The first-order inactivation rate was determined as described under "Materials and Methods." Results are presented using a double logarithmic scale. Closed circles, wild type CelD; open circles, CelD-C*. Error bars indicate the 95% confidence interval for each determination. Ca^{2+} was removed from wild type CelD by treating with Chelex-100 and from CelD-C* by diluting into Chelex-100-treated buffer (contribution of Ca^{2+} initially bound to the enzyme added to the assay was $< 1.5 \times 10^{-7} \text{ M}$). Except for the EGTA-treated samples, all samples contained $1 \mu\text{M}$ ZnCl_2 in addition to the Ca^{2+} concentrations indicated.

The fact that Ca^{2+} binding to site C enhanced the substrate binding affinity and stabilized the conformation of the catalytic site is consistent with the close vicinity of the two sites. The

loop containing the Ca^{2+} -coordinating residues Ser-520, Asp-523, and Ile-525 is connected to the substrate-binding residues His-516 and Arg-518. His-516 and Arg-518 formed hydrogen bonds with hydroxyl groups of the inhibitor *o*-iodobenzyl- β -D-cellobioside in the crystal structure of the enzyme-inhibitor complex (6). In addition, chemical modification and mutagenesis studies identified His-516 as an important residue of the catalytic center (20).

The self-association of monomeric CelD-A* and CelD-B* into a high M_r , presumably dimeric form was not correlated with the occupancy of Ca^{2+} -binding sites. For both proteins, addition of Ca^{2+} or EGTA during non-denaturing electrophoresis failed to alter the proportion of the two forms (data not shown). Both forms displayed very similar Ca^{2+} -binding isotherms. Self-association did not seem to influence thermostability nor kinetic parameters (data not shown). However, the compound effects of site A and B mutations on site C precluded a straightforward analysis of the influence of Ca^{2+} on the stability and kinetic properties of the mutant enzymes.

Unlike catalytic residues, none of the residues involved in Ca^{2+} binding is strictly conserved among all catalytic domains of family E cellulases. At present, it is difficult to predict from sequence analysis which of the other members of family E may be stabilized in a similar manner by Ca^{2+} . It would be of interest to know whether the presence of functional Ca^{2+} -binding sites is correlated with the thermostability of the enzymes.

Acknowledgments—We thank Raphaël de Lecubarri for performing cultures in 15-liter fermentors and Marie-Kim Chaveroche for skillful

technical help. We are grateful to Jean-Paul Aubert and Maxime Schwartz for interest and support.

REFERENCES

1. Lamed, R., Setter, E., and Bayer, E. A. (1983) *J. Bacteriol.* **156**, 828–836
2. Lamed, R., Setter, E., Kenig, R., and Bayer, E. A. (1983) *Biotechnol. Bioeng. Symp.* **13**, 163–181
3. Joliff, G., Béguin, P., Juy, M., Millet, J., Ryter, A., Poljak, R., and Aubert, J.-P. (1986) *Bio/Technology* **4**, 896–900
4. Henrissat, B., Claeysens, M., Tomme, P., Lemesle, L., and Mornon, J.-P. (1989) *Gene (Amst.)* **81**, 83–95
5. Gilkes, N. R., Henrissat, B., Kilburn, D. G., Miller, R. C., Jr., and Warren, R. A. J. (1991) *Microbiol. Rev.* **55**, 303–315
6. Juy, M., Amit, A. G., Alzari, P. M., Poljak, R. J., Claeysens, M., Béguin, P., and Aubert, J.-P. (1992) *Nature* **357**, 89–91
7. Henrissat, B. (1993) *Gene (Amst.)* **125**, 199–204
8. Tokatlidis, K., Salamiou, S., Béguin, P., Dhurjati, P., and Aubert, J.-P. (1991) *FEBS Lett.* **291**, 185–188
9. Tokatlidis, K., Dhurjati, P., and Béguin, P. (1993) *Protein Eng.* **6**, 947–952
10. Chauvaux, S., Béguin, P., and Aubert, J.-P. (1992) *J. Biol. Chem.* **267**, 4472–4478
11. Chauvaux, S., Béguin, P., Aubert, J.-P., Bhat, K. M., Gow, L. A., Wood, T. M., and Bairoch, A. (1990) *Biochem. J.* **265**, 261–265
12. Gibson, T. J. (1984) *Studies on the Epstein-Barr Virus Genome. Ph.D. thesis, University of Cambridge, Cambridge*
13. Yanisch-Perron, C., Vieira, J., and Messing, J. (1985) *Gene (Amst.)* **33**, 103–119
14. Maniatis, T., Fritsch, E. F., and Sambrook, J. (1982) *Molecular Cloning: A Laboratory Manual*, Cold Spring Harbor Laboratory, Cold Spring Harbor, NY
15. Laemmli, U. K. (1970) *Nature* **227**, 680–685
16. Meret, S., and Henkin, R. I. (1971) *Clin. Chem.* **17**, 369–373
17. Bradford, M. (1976) *Anal. Biochem.* **72**, 248–254
18. Kretsinger, R. (1980) *CRC Crit. Rev. Biochem.* **8**, 119–174
19. Tokatlidis, K., Dhurjati, P., Millet, J., Béguin, P., and Aubert, J.-P. (1991) *FEBS Lett.* **282**, 205–208
20. Tomme, P., Chauvaux, S., Béguin, P., Millet, J., Aubert, J.-P., and Claeysens, M. (1991) *J. Biol. Chem.* **266**, 10313–10318
21. Kraulis, P. J. (1991) *J. Appl. Crystallogr.* **24**, 946–950